Organic & Biomolecular Chemistry

Cite this: *Org. Biomol. Chem.*, 2011, **9**, 4748

www.rsc.org/obc

COMMUNICATION

Transition states for cysteine redox processes modeled by DFT and solvent-assisted proton exchange†

Craig A. Bayse*

Received 30th March 2011, Accepted 26th April 2011
DOI: 10.1039/c1ob05497j

Oxidation and disulfide coupling of cysteine, processes central to oxidative stress and biochemical signaling, are modeled using DFT and solvent-assisted proton exchange, a method of microsolvation. Calculated barriers are consistent with experimental kinetics and observed product ratios and suggest a dependence on the polarity of the surrounding medium.

Oxidative modification of cellular thiols by reactive oxygen and nitrogen species (ROS/RNS) is central to the prevention of oxidative stress and the promotion of biochemical signal transduction.[1–7] The glutathione (GSH) thiol/disulfide redox couple which buffers the cell against oxidative stress is a key example.[1] As a result, the GSH : GSSG ratio is an important biomarker for the redox state of the cell. Oxidation of redox-sensitive protein cysteine is an additional telltale for oxidative stress: chemical tagging of the sulfenic acid has been developed to map the cellular thiol proteome (or "sulfenome").[8] Oxidative modification of protein Cys is also important for biochemical signal transduction.[2–6] Small ROS/RNS, in particular H_2O_2 and NO, act as messenger molecules to activate or inactivate transcription, molecular chaperones and other vital cellular processes.[9]

A subset of the redox transformations available to Cys and related thiols is shown in Scheme 1. The sulfhydryl CysSH is oxidized by H_2O_2 or other available ROS to the sulfenic acid (–SOH), sulfinic acid ($–SO_2H$) and sulfonic acid ($–SO_3H$) in sequence. Reaction of the sulfenic acid with an equivalent of endogenous thiol, such as glutathione or protein-bound Cys (either intra- or intermolecularly), generates the disulfide linkage to deactivate the protein by blocking the active site and/or inducing a change in protein conformation. In the absence of an available thiol, CysSOH may condense with a nearby amide to form a cyclic sulfenamide (not shown). Conversion to the sulfenic acid, sulfenamide or disulfide is reversible by thiol reduction and protects against over-oxidation to the sulfinic and sulfonic acids. These higher oxidation states are generally resistant to reduction with the peroxiredoxins as a notable exception.[10] These thiol redox processes are under continued investigation for their role in signal transduction and the prevention of oxidative stress.

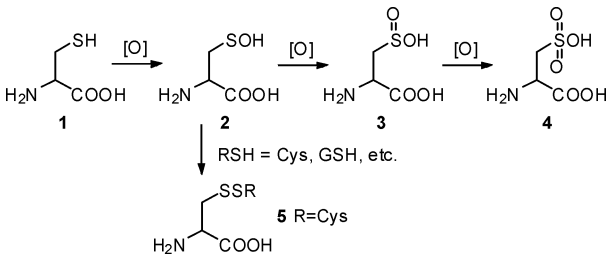

Scheme 1 Mechanism of sequential oxidation and disulfide coupling of cysteine oxidation.

In this communication, we use density-functional theory (DFT) and solvent-assisted proton exchange (SAPE) to explore the oxidation and disulfide coupling of Cys. The SAPE method uses explicit solvation to facilitate proton transfer pathways to approximate the action of bulk solvent in a gas-phase computational model. Similar microsolvation methods have been used by various groups to model aqueous phase reactivity.[11,12] For the Cys redox pathways in Scheme 1, transition states were determined using the SAPE networks shown in Scheme 2. In these models, two or more water molecules were added to an initial complex of reactants such that progress of the heavy atoms along the reaction coordinate was coupled to transfer of H^+ through the water network. (See the ESI for additional discussion and details of model design).† Our previous work on the related redox chemistry of selenium using SAPE models produced activation barriers consistent with experimental observations and significantly lower than those computed from models using direct, non-solvent-mediated proton transfer.[11]

Oxidation of **1** by MeOOH was modeled using a two-water SAPE network as the heterolytic cleavage of the O–O bond with OH^+ transfer to the sulfur center (Scheme 2a). Within this model, proton transfer through the SAPE network is driven by the negative charge that accumulates on the MeO^-. As shown in Fig. 1a, the transition state shows significant motion of the protons through the SAPE network concurrent with O–O bond cleavage (Δd(O–O) = +0.3 Å) and –OH group transfer to sulfur (d(S–O) = 2.31 Å). The long S–H bond (1.72 Å) indicates that the thiol is largely deprotonated at the transition state consistent with the pH dependence observed experimentally.[13] The SAPE activation enthalpy ($\Delta H^‡$ = 17.0 kcal mol^{-1}) for this model is similar to the experimental value determined by temperature-dependent kinetics studies (16.4 ± 0.3 kcal mol^{-1}) for oxidation of **1** by H_2O_2 conducted

Department of Chemistry and Biochemistry, Old Dominion University, Norfolk, Virginia, United States. E-mail: cbayse@odu.edu; Fax: +1 757 683 4628; Tel: +1 757 683 4097

† Electronic supplementary information (ESI) available: Theoretical methods. See DOI: 10.1039/c1ob05497j

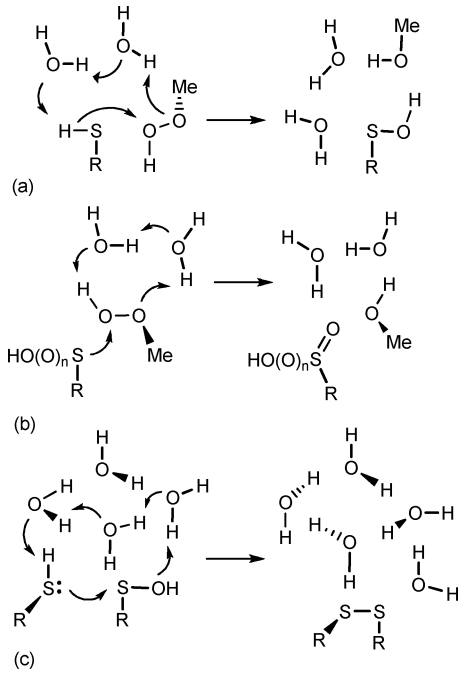

Scheme 2 SAPE models for cysteine oxidation: (a) thiol oxidation, (b) oxygen atom transfer to sulfi(o)nic acid (n = 0, 1), (c) disulfide bond formation.

at pH 6 where the sulfhydryl is in the neutral form.[13] In the product complex (Fig. 1a), the sulfenic acid forms a hydrogen bond to the carboxylic acid group. This conformation is maintained for subsequent oxidation steps.

Rates of thiol oxidation are highly pH-dependent and roughly correlate to the sulfhydryl pK_a.[14] Deprotonation of the thiol increases the nucleophilicity of the sulfur center and many redox-sensitive Cys residues are located in polar active sites and stabilized by acidic residues.[15] An alternate model for oxidation of the thiolate **1**$^-$ was constructed to include an extended SAPE network to accommodate explicit solvation of the anion (Fig. 1b). For this cubic SAPE network, the proton is transferred from the –COOH group to the evolving methoxide through the water molecule on the lower half of the cube (product = $H_2NCH(COO^-)CH_2SOH$ **2**$^-$). The carboxylic acid was maintained in the acid form in spite of its lower pK_a to avoid a high negative charge in the DFT model. The $\Delta G^‡$ for this model is ~6 kcal mol^{-1} lower than for CysSH oxidation and earlier along the reaction coordinate (d(O–O) = 1.70 Å; d(S–O) = 2.49 Å). This difference in activation barriers is roughly consistent with the 100-fold increase in rate at high pH.[13]

Over-oxidation of **2** to **3** and **4** was modeled using a two-water network in which oxygen atom transfer to sulfur is concurrent with an intramolecular proton transfer (Scheme 2b). The transition states for these processes (Fig. 1c–d) occur at similar O–O distances (~1.96 Å), but at a shorter S–O distance for **3** oxidation (1.84 Å *vs.* 1.94 Å). This 'later' transition state is in agreement with the higher activation barrier for the sulfinic acid (Table 1). For these oxidation steps, COSMO solvation corrections were calculated in water, chlorobenzene and cyclohexane to represent a highly polar, moderately polar and nonpolar protein environment, respectively. Whereas initial oxidation of the sulfhydryl or thiolate is largely independent of the solvent environment (ΔG_{solv} < 2 kcal mol^{-1}), oxidation to **3** and, to a lesser extent, **4**, are sensitive to the polarity of the solvent environment. These results agree with experimental conclusions about conditions favorable for modification of protein-bound Cys.[15] Highly polar environments stabilize the accumulation of charge at the transition state to reduce the barrier for **2** oxidation by ~5.5 kcal mol^{-1} favoring over-oxidation of Cys in surface sites exposed to the solvent or adjacent to polar residues. Computational studies of the reduction in thioredoxin disulfides also show a dependence on the protein environment.[16]

Disulfide coupling was modeled as the attack of **1** upon **2** to form the S–S bond concurrent with loss of water using a square four-water SAPE network (Scheme 2c). Following the S–S bond formation coordinate from the reactant complex in Fig. 1e, the transition state was found when the S–S distance was reduced to 2.35 Å and the thiol was completely deprotonated (d(S–H = 2.29 Å). The activation barrier in water (12.5 kcal mol^{-1}) is slightly higher than that calculated for reduction of selenenic acid by a thiol (6.6 kcal mol^{-1}) and is reduced in non-polar solvent environments (Table 1). As this barrier is relative to the donor–acceptor complex of **1** with the sulfenic acid (d(S···S) = 3.35 Å), additional barriers, such as peptide rearrangement, must also be overcome for disulfide bond formation. Note that the SAPE model, as well as microsolvation studies of reactions at disulfides,[17a] predicts nucleophilic substitution to proceed by an S_N2-type mechanism in contrast to purely gas-phase models which prefer a stepwise addition–elimination.[17b] The rate of disulfide formation would be rapid in cases where the thiol is in close proximity to **2**, the concentration of thiol is high or polar groups activate the thiol and/or sulfenic acid. Relative DFT-SAPE activation barriers for **1** oxidation and disulfide formation are consistent with kinetics studies by Luo *et al.* in which **5** is the major product at [H_2O_2] : [Cys] ratios below 10 : 1, but over-oxidation predominates at higher peroxide concentrations.[13]

Table 1 DFT(B3PW91)-SAPE Gibbs free energies (kcal mol^{-1}) for cysteine redox processes

Reaction	$\Delta H^‡$	$\Delta G^‡$	$\Delta G^‡ + \Delta G_{solv}$	ΔG_{rxn}
1 + MeOOH → **2** + MeOH	17.0, *16.4*[a]	21.9	19.1,[b] 20.1,[c] 21.0[d]	–51.3
1$^-$ + MeOOH → **2**$^-$ + MeOH	12.5	14.0	13.9,[b] 14.6,[c] 14.3[d]	–44.5
2 + MeOOH → **3** + MeOH	21.9	21.1	15.6,[b] 17.3,[c] 19.2[d]	–50.8
3 + MeOOH → **4** + MeOH	28.3	28.0	24.7,[b] 25.6,[c] 26.8[d]	–57.8
1 + **2** → **5** + H_2O	3.7	8.3	12.5,[b] 11.1,[c] 9.7[d]	–27.5

[a] Exp; oxidant = H_2O_2 (ref. 13); COSMO correction for bulk solvation in: [b] water, [c] PhCl, [d] C_6H_{12}.

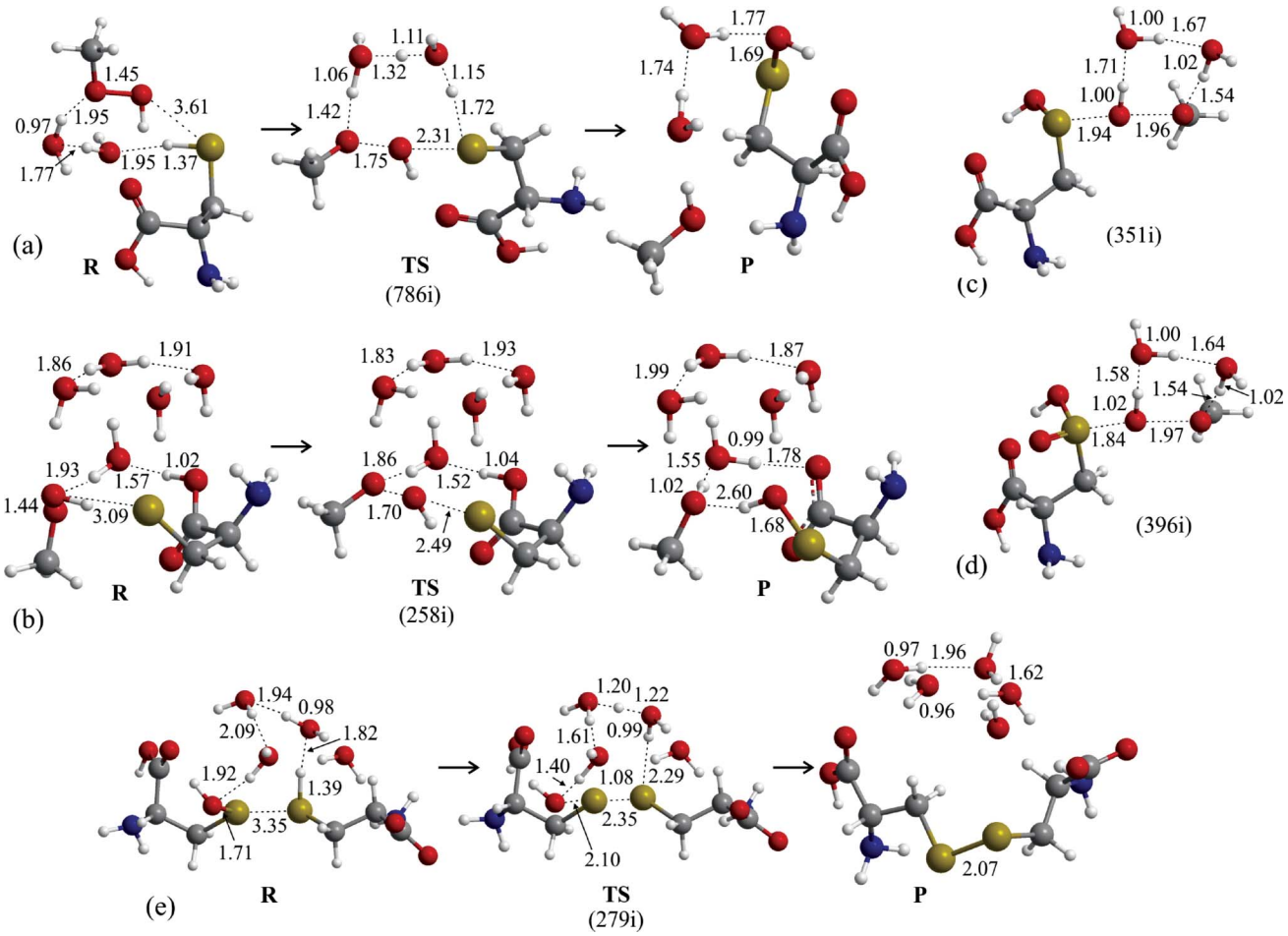

Fig. 1 Selected bond distances (Å) for the reactants (R), transition states (TS) and products (P) of the SAPE models of MeOOH oxidation of (a) **1** to **2**, (b) $\mathbf{1}^-$ to $\mathbf{2}^-$, (c) **2** to **3** (TS only), and (d) **3** to **4** (TS only); and (e) **5** formation from **1** and **2**. Imaginary frequencies are given for each TS.

Conclusions

Gas-phase SAPE models incorporating a representation of the role of solvent in proton exchange show that oxidation of Cys to the sulfenic acid and disulfide formation are relatively low barrier processes. Interactions with residues surrounding a protein-bound Cys and not present in the models above may stabilize either the reactant or transition state to modify the activation barrier. Further oxidation to the sulfinic or sulfonic acids, likely occur under higher conditions of oxidative stress, are dependent upon the surrounding environment. Over-oxidation is predicted to be more favorable in polar environments such that Cys may be protected from irreversible oxidation if located in a hydrophobic pocket. The agreement between the DFT-SAPE models and experimental conclusions about the stabilization of sulfenic acids by certain protein environments[15] and observed activation barriers and product distributions[13] is an important step toward understanding the role of sulfur redox chemistry in biological processes.

This work was funded by the National Science Foundation (CHE-0750413).

Notes and references

1 F. Q. Schafer and G. R. Buettner, *Free Radical Biol. Med.*, 2001, **30**, 1191–1212.
2 A. Claiborne, J. I. Yeh, T. C. Mallett, J. Luba, E. J. Crane, V. Charrier and D. Parsonage, *Biochemistry*, 1999, **38**, 15407–15415.
3 A. Bindoli, J. M. Fukuto and H. J. Forman, *Antioxid. Redox Signaling*, 2008, **10**, 1549–1564.
4 D. Barford, *Curr. Opin. Struct. Biol.*, 2004, **14**, 679–686.
5 J. V. Cross and D. J. Templeton, *Antioxid. Redox Signaling*, 2006, **8**, 1819–1827.
6 L. B. Poole and K. J. Nelson, *Curr. Opin. Chem. Biol.*, 2008, **12**, 18–24.
7 K. G. Reddie and K. S. Carroll, *Curr. Opin. Chem. Biol.*, 2008, **12**, 746–754.
8 (*a*) Y. H. Seo and K. S. Carroll, *Proc. Natl. Acad. Sci. U. S. A.*, 2009, **106**, 16163–16168; (*b*) S. E. Leonard, K. G. Reddie and K. S. Carroll, *ACS Chem. Biol.*, 2009, **4**, 783–799.
9 H. J. Forman, J. Fukuto and M. Torres, *Signal Transduction by Reactive Oxygen and Nitrogen Species*, Kluwer, Dordrecht, 2003.
10 (*a*) B. Biteau, J. Labarre and M. B. Toledano, *Nature*, 2003, **425**, 980–984; (*b*) C. Jacob, A. L. Holme and F. H. Fry, *Org. Biomol. Chem.*, 2004, **2**, 1953–1956.
11 (*a*) C. A. Bayse, *J. Phys. Chem. A*, 2007, **111**, 9070–9075; (*b*) C. A. Bayse and S. Antony, *J. Phys. Chem. A*, 2009, **113**, 5780–5785; (*c*) C. A. Bayse, *J. Inorg. Biochem.*, 2010, **104**, 1–8.
12 Selected examples: (*a*) B. Kallies and R. Mitzner, *J. Mol. Model.*, 1998, 4, 183; (*b*) C. S. Yeung, P. L. Ng, X. Guan and D. L. Phillips, *J. Phys. Chem. A*, 2010, **114**, 4123–4130; (*c*) S. Yamabe, N. Tsuchida and S. Yamazaki, *J. Phys. Chem. A*, 2010, **114**, 11699–11707; (*d*) L. Gorb, A. Asensio, I. Tunon and M. F. Ruiz-Lopez, *Chem.–Eur. J.*, 2005, **11**, 6743–6753; (*e*) J. I. Mujika, J. M. Mercero and X. Lopez, *J. Am. Chem. Soc.*, 2005, **127**, 4445–4453.

13 D. Luo, S. W. Smith and B. D. Anderson, *J. Pharm. Sci.*, 2005, **94**, 304–316.
14 C. C. Winterbourn and D. Metodiewa, *Free Radical Biol. Med.*, 1999, **27**, 322–328.
15 A. Claiborne, H. Miller, D. Parsonage and R. P. Ross, *FASEB J.*, 1993, **7**, 1483–1490.
16 A. T. P. Carvalho, P. A. Fernandes, M. Swart, J. N. P. van Stralen, F. M. Bickelhaupt and M. J. Ramos, *J. Comput. Chem.*, 2009, **30**, 710–724.
17 (*a*) J. M. Hayes and S. M. Bachrach, *J. Phys. Chem. A*, 2003, **107**, 7952–7961; (*b*) S. M. Bachrach and D. C. Mulhearn, *J. Phys. Chem. A*, 1996, **100**, 3535–3540.